PHYSICAL REVIEW B **69**, 121401(R) (2004)

Defect-induced gap states in Al_2O_3 thin films on NiAl(110)

Niklas Nilius, Maria Kulawik, Hans-Peter Rust, and Hans-Joachim Freund
Fritz-Haber Institut der MPG, Faradayweg 4-6, D-14195 Berlin, Germany
(Received 21 October 2003; published 8 March 2004)

The electronic properties of one-dimensional defects in ultrathin Al_2O_3 films have been investigated by low-temperature STM and STS. Whereas line defects between two oxide domains show almost no topographic contrast in low bias images, they appear with a distinct corrugation at higher positive sample bias. Conductance spectroscopy and imaging reveal three unoccupied states at +2.5, +3.0, and +4.5 V localized along the domain boundaries. The defect-induced states are responsible for the observed contrast variation and originate most likely from a nonstoichiometric oxide composition at the interface between two Al_2O_3 domains.

DOI: 10.1103/PhysRevB.69.121401 PACS number(s): 73.20.Hb, 76.30.Mi, 68.47.Gh, 68.37.Ef

Ionic oxides are usually optically transparent, chemically inert, and good electric insulators, due to their large band gaps between occupied and unoccupied states. Defects in the oxide structure cause deviations from this idealized behavior and decisively influence the properties of real oxides.[1] The presence of oxygen vacancies or impurity atoms induces strong modifications in the optical behavior of oxide crystals, forming the basis for several laser applications.[2] Defect-induced chemical activation was observed for the dissociation of water on O vacancies in a TiO_2 (110) surface.[3] Also the reduction of NiO in a hydrogen atmosphere requires the presence of point defects in the oxide surface.[4]

Theoretical investigations of simple defects, such as O vacancies, already provide good insights into their geometric and electronic structure.[5–9] The absence of a lattice atom induces discrete energy levels in the oxide band gap, occupied by one or two electrons. Such F and F^+ color centers have been identified by optical absorption and electron spin resonance spectroscopy, whereby the latter method sensitively detects unpaired electrons trapped in the defect states.[2,10] The knowledge on more complex, one- and two-dimensional defects is rather scarce, although they play a decisive role in nucleation and the growth of metal overlayers on oxide surfaces.[11–13] The influence of Al_2O_3 line defects on energy levels of single, adsorbed Pd atoms has recently been demonstrated by scanning tunneling microscopy (STM) and spectroscopy (STS).[14]

A detailed investigation of geometric and electronic properties of oxide defects is complicated by their irregular structure and statistical arrangement, which strongly limits the use of nonlocal surface science techniques. On the other hand, a local probe such as STM requires a conductive sample and is therefore not applicable for insulating bulk oxides. The problem can be circumvented by the use of ultrathin oxide layers grown on a metal surface, which are transparent for low-energy electrons and therefore suited for electron- and ion-mediated experimental techniques. A good representation of the respective bulk oxides have been found for thin films of Al_2O_3 on $Ni_3Al(111)$ and NiAl(110), SiO_2 on Mo(211) or MgO on W(100).[13,15–18]

This paper focuses on the electronic characterization of line defects formed between domains of a crystalline Al_2O_3 film grown on NiAl(110). Low-temperature STS revealed the presence of unoccupied gap states induced by the domain boundaries. The electronic properties were connected to the atomic structure of the line defects, which is known from earlier measurements.[19]

The experiments were performed in an UHV-STM operating at 4 K. The NiAl(110) substrate was cleaned by alternating cycles of Ar^+ sputtering and annealing to 1000 °C. The crystal was then exposed to 1000 L of O_2 at 280 °C and healed for 5–7 min at 800 °C. The procedure results in the formation of a crystalline Al_2O_3 thin film, whose quality was controlled by low-energy electron diffraction (LEED) and STM measurements. The main characteristics of the Al_2O_3 layer have already been described in detail and are only summarized in the following paragraph.[18–24] The film consists of two Al-O layers with a total thickness of approximately 5 Å. Its valence band is mainly composed from O $2p$ orbitals, whereas Al $3s$ levels dominate the conduction band. The gap between occupied and unoccupied states in the oxide layer was determined by electron energy loss spectroscopy and photoelectron/x-ray absorption spectroscopy to be roughly 8 eV and is only slightly smaller than in bulk alumina. Due to the twofold symmetry of the NiAl support, the film grows in two reflection domains A and B, tilted by $\pm 24.1°$ with respect to the NiAl $[1\bar{1}0]$ direction. The domains are separated by a network of line defects, namely reflection domain boundaries between opposite domains (A-B) and antiphase domain boundaries between equivalent domains (A-A, B-B). Antiphase domain boundaries have a well-defined atomic structure, resulting from the insertion of an additional row of oxygen atoms between two neighboring oxide unit cells.[19] The additional row in the topmost oxide layer is inserted either along the short unit cell vector, forming a straight boundary, or along the diagonal of the Al_2O_3 cell, causing a zigzagged dislocation line. In contrast, reflection domain boundaries show no order on the atomic scale and run in arbitrary directions. The local disorder leads to a less-defined electronic structure, which is why this defect type will be disregarded in the following discussion. However, general electronic properties were found to be similar for reflection and antiphase domain boundaries.

The apparent height of antiphase domain boundaries shows distinct variations as a function of sample bias in STM topographic images (Fig. 1).[24] At negative and small positive bias (-3.5 V to $+1.0$ V), the height contrast to surrounding undisturbed oxide patches is negligible and line

0163-1829/2004/69(12)/121401(4)/$22.50 ©2004 The American Physical Society

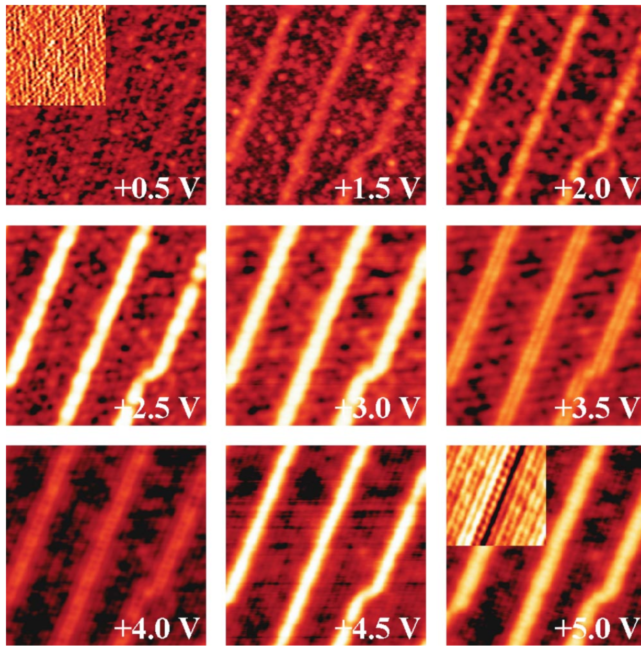

FIG. 1. (Color online) STM topographic images of straight antiphase domain boundaries on Al_2O_3/NiAl(110) taken at the indicated sample bias (image sizes 300×300 Å, $I=0.1$ nA). Differentiated and contrast-enhanced sections of two images are shown in the insets.

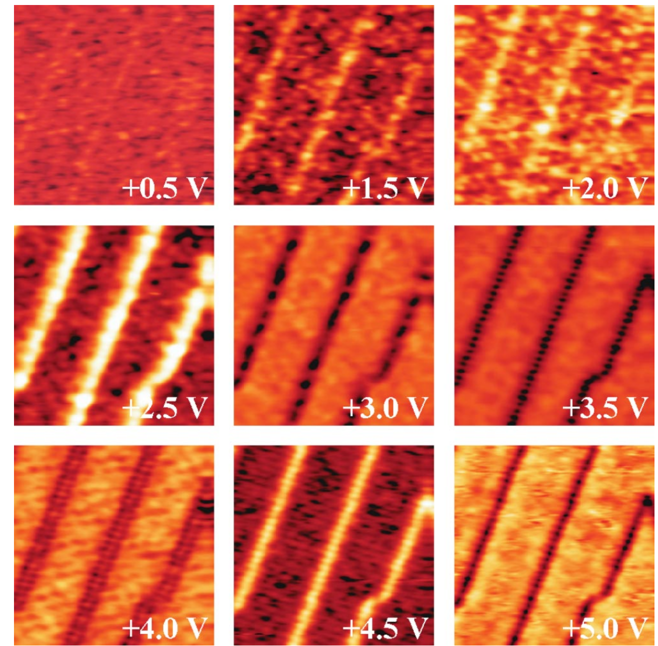

FIG. 2. (Color online) Conductance (dI/dV) images of the antiphase domain boundaries on Al_2O_3/NiAl(110), which are shown in Fig. 1. The images were taken at the indicated sample bias and are scaled to the same dI/dV intensity (image sizes 300×300 Å, $I=0.1$ nA).

defects are almost invisible in the STM. In images taken around zero bias, the domain boundaries are only identified by the deviating atom positions compared to their arrangement in regular oxide unit cells.[19] Above +1.5 V, the antiphase domain boundaries appear as bright lines in topographic images. Their apparent height gradually increases with increasing sample bias and peaks at approximately +2.5 V. Applying higher positive voltages slightly reduces the topographic contrast. However, the one-dimensional defects are imaged as protruding lines for voltages as high as +6.0 V. The bias-dependent corrugation of line defects is summarized in Fig. 3. Contrast variations between antiphase domain boundaries and regular oxide patches are accompanied by changes in the geometric pattern. Between +1.5 and +3.0 V, the boundaries are imaged as single white lines. They become double strands with a groovelike depression in the center between +3.5 and +4.0 V and narrow down to a single line in images taken above +4.5 V. Bias-dependent variations in the topographic pattern are also observed on regular oxide domains (Fig. 1 insets). The zigzag structure visible in low bias images was earlier assigned to a reconstruction in the quasihexagonal arrangement of the topmost O atoms. At higher positive voltage, the zigzag pattern transforms into a series of parallel double lines with one line pair per oxide unit cell.

The observed bias-dependent height of Al_2O_3 domain boundaries points to a dominance of electronic versus topographic effects in STM images. This assumption is supported by the vanishing corrugation of line defects at very low sample bias. In such a case, the height response of the STM tip to maintain a constant tunnel current reflects the averaged local density of states (LDOS) of the sample surface. For tunneling into the Al_2O_3 band gap, the tunneling matrix elements are still influenced by oxide states but additionally represent the LDOS at the metal-oxide interface. Images at relatively small voltages show consequently an intermixture between the reconstructed topmost oxide layer and the NiAl surface (Fig. 1, upper left inset). Above +3.0 V sample bias, the Al-induced conduction band provides most of the final states for tunneling electrons. The double line structure observed on regular oxide domains is therefore indicative of a linear arrangement of Al ions, which form chains along the short unit cell vector of the Al_2O_3 film.[25] The distinct contrast maximum of domain boundaries in STM images taken at 2.5 V points to the presence of gap states localized along the oxide line defects.

Whereas constant current topographies average over the LDOS between the tip and sample Fermi level, differential conductance (dI/dV) measurements exclusively probe states with an energy close to the applied bias voltage. The dI/dV signal gives, therefore, a much better evaluation of the LDOS of the sample surface. Figure 2 shows conductance images of oxide line defects, simultaneously measured with the topographic images from Fig.1. In accordance to STM topographies, dI/dV images of domain boundaries show little contrast with respect to regular oxide patches at negative and small positive voltages. For a sample bias above +1.5 V, the dI/dV signal on line defects strongly increases and passes through a pronounced maximum at +2.5 V. The dI/dV peak reproduces the maximum in apparent height, but shows a much smaller width due to the better energy resolu-

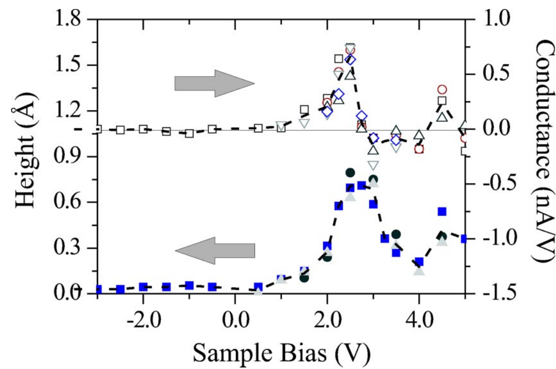

FIG. 3. (Color online) Bias dependence of apparent height and dI/dV intensity of antiphase domain boundaries with respect to defect-free Al_2O_3 domains on NiAl(110). The symbols show results from different experimental runs; the broken lines represent the best fit through the data points. The two maxima indicate defect states induced by the domain boundaries.

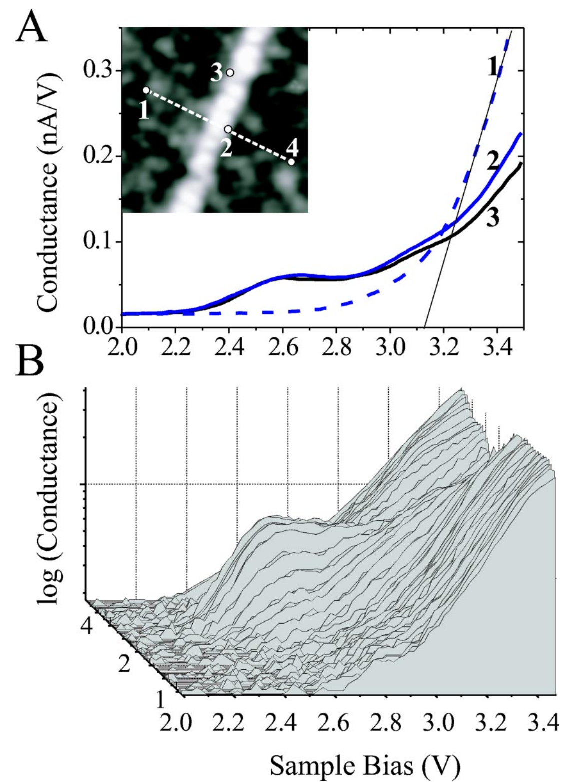

FIG. 4. (Color online) (a) Conductance spectra taken on a straight antiphase domain boundary and a regular region of Al_2O_3/NiAl(110). The solid line interpolates the onset of the Al_2O_3 conduction band. (b) Series of 70 dI/dV spectra taken across a domain boundary. The corresponding tip positions are marked in the inset of (a). To emphasize the additional dI/dV peaks at the line defect, a logarithmic scale is used in the diagram. The gap was set with $U_{sample}=3.0$ V and $I=0.1$ nA in both cases.

tion of the differential measurement (Fig. 3). Above +2.5 V, the dI/dV intensity of line defects attenuates and drops below the value of regular oxide domains. As a result, the domain boundaries appear as depressions in dI/dV images taken around +3.5 V. A further conductance maximum was detected at +4.5 V, indicating a second unoccupied state induced by the Al_2O_3 line defects. Also in dI/dV images, the observed defect pattern changes as a function of sample bias, from a single line below +3.0 V to a double strand around +4.0 V and back to a single line at higher energy.

Supplementary information on the electronic structure of oxide domain boundaries on Al_2O_3/NiAl(110) was gained by dI/dV spectroscopy. Here the tip is stabilized on a selected position and the bias-dependent dI/dV signal is measured with lock-in technique disabled feedback loop. In contrast to dI/dV imaging, the tip height is constant during spectroscopy and the conductance is not influenced by a varying tip-sample separation. Figure 4(a) shows two dI/dV spectra of an antiphase domain boundary in comparison to a spectrum taken above a regular oxide region. In distance to the line defect, the conductance steadily rises with applied sample bias. The kink in the dI/dV curve around +3.1 V marks the onset of the Al_2O_3 conduction band. For tip positions above a domain boundary, a pronounced dI/dV peak around +2.6 V appears in the spectra, flanked by a smaller maximum at +3.0 V. At higher voltages, the dI/dV intensity falls behind the value measured away from the line defect, which causes the negative contrast of domain boundaries in the respective dI/dV images. The +4.5 V peak observed by dI/dV imaging could not be detected in the spectroscopic mode, because it is covered by the sharply increasing conductance above 3.1 V. A series of 70 dI/dV spectra taken across a line defect clearly demonstrates the development of defect states in the vicinity of antiphase domain boundaries [Fig. 4(b)].

The investigations of the local electronic properties of a Al_2O_3 thin film consistently show the presence of gap states induced by the one-dimensional defects. Two pronounced states at +2.5 and +4.5 V were identified by topographic and dI/dV imaging. An additional shoulder in the LDOS at +3.0 V showed up only in dI/dV spectroscopy due to its better energy resolution. The observed level energies are influenced by the tip-induced electric field, which bends the oxide bands in dependence of the actual tip-sample distance. Due to the high dielectric constant of alumina and the small thickness of the oxide film, the level shifts are supposed to be small. The detected defect levels are generally unoccupied. Taking the kink at +3.1 V in dI/dV spectra of the regular oxide as a fingerprint of the conduction-band edge, the +2.5 V defect state clearly lies inside the Al_2O_3 band gap. The higher levels are close to or already above the conduction-band edge. From bias-dependent changes in the geometric pattern of domain boundaries, the spatial localization of defect states can be derived. The level at +2.5 V shows up as a single line in STM images and is therefore relatively localized along the dislocation line. In the energy region of the higher levels, a double line is imaged in topographic and dI/dV modes, separated by a region of reduced LDOS. The existence of a nodal plane in the center of the boundary could be indicative for a p-like symmetry of the underlying defect states.

The limited knowledge on complex defects in Al_2O_3 thin films complicates a comprehensive interpretation of the data.

The defect states associated with isolated O vacancies have been extensively studied in bulk alumina using optical absorption and electron spin resonance spectroscopy,[2,10] as well as various theoretical approaches.[8,9] An occupied s-like ground state was found 3 eV above the valence-band minimum and three unoccupied p-like states form close to the conduction-band edge. The latter, unoccupied levels show similar properties as defect states observed along the Al_2O_3 domain boundaries. In analogy to Al_2O_3 units containing a single oxygen vacancy, line defects in the thin film may represent a local nonstoichiometric and oxygen-deficient structure. In contrast to isolated vacancies, the neighboring defect levels along domain boundaries couple and probably broaden to a bandlike structure with enhanced width. In discrepancy to the Al_2O_3 point defects, no occupied ground state could be observed along the line defects in the present experiments. The detection of low-lying occupied states is generally difficult with STS due to the exponential decay in tunneling probability with separation from the Fermi level and the localized character of deeper levels. In another scenario, the absent occupied level in the gap might be the consequence of the small film thickness, allowing a charge transfer from oxide states to the underlying NiAl substrate.

The nature of defect states induced by domain boundaries in Al_2O_3/NiAl(110) cannot be unraveled from the present experimental data alone. The information on local structural and electronic properties of line defects may, however, stimulate new theoretical efforts for a detailed characterization of complex oxide defects. The interest for extended defects is motivated by their strong interaction with deposited metal atoms, which determines the growth of metals on oxide surfaces. A better understanding and control over these interactions would have considerable impact on technologies using metal-oxide interfaces, such as heterogeneous catalysis and semiconductor techniques.

[1] C. Noguera, *Physics and Chemistry at Oxide Surfaces* (Cambridge University Press, Cambridge, 1996); P. A. Cox, *Transition Metal Oxides* (Clarendon Press, Oxford, 1992).

[2] M. Ghamnia, C. Jardin, L. Martinez, M. Bouslama, and P. Durupt, Vacuum **48**, 129 (1997).

[3] R. Schaub, P. Thostrup, N. Lopez, E. Laegsgaard, I. Stensgaard, J. K. Norskov, and F. Besenbacher, Phys. Rev. Lett. **87**, 266104 (2001).

[4] J. A. Rodriguez, J. C. Hanson, A. I. Frenkel, J. Y. Kim, and M. Perez, J. Am. Chem. Soc. **124**, 346 (2002).

[5] V. Nasluzov, V. Rivanenkov, A. Gordienko, K. Neyman, U. Birkenheuer, and N. Roesch, J. Chem. Phys. **115**, 8157 (2001).

[6] T. Bredow and G. Pacchioni, Chem. Phys. Lett. **355**, 417 (2002).

[7] C. Jun, L. Lin, and L. Yong, Eur. Phys. J. B **9**, 593 (1999).

[8] A. Stashans, E. Kotomin, and J.-L. Calais, Phys. Rev. B **49**, 14 854 (1994).

[9] Y.-N. Xu, Z.-Q. Gu, X-F. Zhong, and W. Y. Ching, Phys. Rev. B **56**, 7277 (1997).

[10] G. Pacchioni, Solid State Sci. **2**, 161 (2000) and references therein.

[11] C. R. Herny, Surf. Sci. Rep. **31**, 231 (1998).

[12] G. Haas, A. Menck, H. Brune, J. V. Barth, J. A. Venables, and K. Kern, Phys. Rev. B **61**, 11 105 (2000).

[13] M. Bäumer and H.-J. Freund, Prog. Surf. Sci. **61**, 7 (1997).

[14] N. Nilius, T. M. Wallis, and W. Ho, Phys. Rev. Lett. **90**, 046808 (2003).

[15] A. Rosenhahn, J. Schneider, C. Becker, and K. Wandelt, Appl. Surf. Sci. **142**, 169 (1999).

[16] T. Schroeder, M. Adelt, B. Richter, M. Naschitzki, M. Bäumer, and H.-J. Freund, Surf. Rev. Lett. **7**, 7 (2000).

[17] S. C. Street, C. Xu, and D. W. Goodman, Annu. Rev. Phys. Chem. **48**, 43 (1997).

[18] R. Franchy, Surf. Sci. Rep. **38**, 195 (2000).

[19] M. Kulawik, N. Nilius, H.-P. Rust, and H.-J. Freund, Phys. Rev. Lett. **91**, 256101 (2003).

[20] R. M. Jaeger, H. Kuhlenbeck, H.-J. Freund, M. Wuttig, W. Hoffmann, R. Franchy, and H. Ibach, Surf. Sci. **259**, 235 (1991).

[21] R. M. Jaeger, J. Libuda, M. Bäumer, K. Homann, H. Kuhlenbeck, and H.-J. Freund, J. Electron Spectrosc. Relat. Phenom. **64**, 217 (1993).

[22] S. Andersson, P. A. Brühwiler, A. Sandell, M. Frank, J. Libuda, A. Giertz, B. Brena, A. J. Maxwell, M. Bäumer, H.-J. Freund, and N. Martensson, Surf. Sci. **442**, L964 (1999).

[23] G. Ceballos, Z. Song, J. I. Pascual, H.-P. Rust, H. Conrad, M. Baeumer, and H.-J. Freund, Chem. Phys. Lett. **359**, 41 (2002).

[24] K. Højrup Hansen, T. Worren, E. Lægsgaard, F. Besenbacher, and I. Stensgaard, Surf. Sci. **475**, 76 (2001).

[25] From phonon spectra measured with HREELS, the coexistence of octahedral and tetrahedral Al ions was determined for the Al_2O_3 film on NiAl(110). Alternating rows of octahedral and tetrahedral coordinated Al ions provide a possible explanation for the observed double lines in the oxide unit cell, in accordance with model calculations presented in D. R. Jennison and A. Bogicevic, Surf. Sci. **464**, 108 (2000).